Marine Geology 386 (2017) 32–43

Contents lists available at ScienceDirect

Marine Geology

journal homepage: www.elsevier.com/locate/margo

Shoal morphodynamics of the Changjiang (Yangtze) estuary: Influences from river damming, estuarine hydraulic engineering and reclamation projects

Wen Wei [a], Zhijun Dai [a,*], Xuefei Mei [a], J. Paul Liu [b], Shu Gao [a], Shushi Li [a,c]

[a] State Key Lab of Estuarine & Coastal Research, East China Normal University, Shanghai 200062, China
[b] Department of Marine, Earth, and Atmospheric Sciences, North Carolina State University, Raleigh, NC, USA
[c] Key Laboratory of Coastal Science and Engineering, Qinzhou University, Qinzhou, Guangxi 535099, China

ARTICLE INFO

Article history:
Received 29 November 2016
Received in revised form 13 February 2017
Accepted 20 February 2017
Available online 22 February 2017

Keywords:
Shoal morphodynamics
Tidal channel infilling
Estuarine hydraulic engineering
Reclamation
Three Gorges Dam
Changjiang Estuary

ABSTRACT

Concerns regarding estuarine shoal morphodynamics have increased worldwide because of intensive anthropogenic activities. To explore response of estuarine shoals to possible couplings of multiple artificial interferences in river basins and within estuaries, the link between the morphodynamic processes of the Nanhui Shoal (NHS), which is located along the southern margin of the Changjiang estuary, the largest estuary in Asia, and river damming, estuarine hydraulic engineering and reclamation projects, is discerned in this study. The results reveal that the NHS exhibited secular polarization during 1998–2013, with a significant accretion of 1.8×10^8 m^3 landward from the tidal ridge and an erosion of 0.3×10^8 m^3 on the seaward edge, respectively, forming a steep slope with an elevation between −2 and −3 m. Meanwhile, the NHS morphodynamics could be divided into 3 stages: mild accretion with an undisturbed tidal channel during 1998–2002, strong sedimentation with a disrupted tidal channel during 2003–2008, and large-scale landward accretion with an infilled tidal channel after 2009. Moreover, the NHS's volume variations exhibited an 18-month cycle, even though an increased area of 35 km^2 above −2 m and a decreased area of 45 km^2 between −2 and −5 m were observed. The primary causes of theses periodic changes in the NHS's volume are determined as the fluctuating Changjiang water discharge and cyclically altered hydrodynamics of the South Passage. The Deep Waterway Project (DWP) and reclamation projects were responsible for the polarization of seaward erosion and landward accretion, respectively. Moreover, these reclamation projects dominated the staggered changes in NHS morphodynamics by inducing continuous accretion within the tidal channel. Compared to estuarine engineering, river damming induced dramatic declines in distal sediment may have played a minor role in flat changes of NHS.

1. Introduction

Estuarine shoals, which are located at transition zone between rivers and oceans, act as vital habitats for living creatures and reserve land resources for urban sprawl, especially in developing countries with increasing urbanization and exploding populations (Dyer et al., 2000; Kim, 2010). However, estuarine shoals have experienced dramatic changes because of intensified human activities from upstream basin and estuary itself in the most recent decades, even though these regions could provide precious benefits, such as storm protection and hazard mitigation for cities (Lafite and Romaña, 2001; Anthony et al., 2014; van der Werf et al., 2015).

Basin-wide human activities, especially damming, could sharply decrease the amount of suspended sediment delivering to estuaries, which could trigger sediment starvation and the subsequent erosion of estuarine shoals and subaqueous deltas (Syvitski et al., 2005; Blum and Roberts, 2009; Anthony et al., 2015). In the Mississippi estuary, more deltaic shoals would become submerged if the riverine sediment input decreases by 50% through dam construction (Blum and Roberts, 2009). The retention of riverine suspended sediment by dams has also contributed to the large-scale shoal erosion and land loss of the Mekong Delta (Anthony et al., 2015). However, discrepancies exist in estuaries where no significant erosion trends were detected despite lower riverine sediment load. For instance, the estuarine shoal accretion rate in the Keum Estuary (Korea) significantly increased, even though the riverine loads decreased sharply because of dam construction (Kim et al., 2006). The estuarine shoal region in the Changjiang Estuary experienced continuous accretion despite damming induced declines in riverine sediment (Luan et al., 2016).

While river damming can sharply decrease the riverine sediment input (Syvitski et al., 2005; Blum and Roberts, 2009; Anthony et al.,

* Corresponding author.
E-mail address: zjdai@sklec.ecnu.edu.cn (Z. Dai).

http://dx.doi.org/10.1016/j.margeo.2017.02.013
0025-3227/

2015), estuarine hydraulic engineering projects, including dredging activity and construction, could also play critical roles in altering estuarine hydrodynamics and controlling estuarine shoal morphodynamics (Lafite and Romaña, 2001; van der Wal et al., 2002). For example, channel dredging in the Ribble Estuary (England) decreased the flow velocities over adjoining estuarine shoals, which induced the accretion of the upper intertidal zone (van der Wal et al., 2002). Similar accretions on both sides of the North Passage in the Changjiang estuary were also observed because of channel projects (Dai et al., 2013). Meanwhile, considerable accretion was detected in the entire estuary of the Lune River (England) owning to construction of seawalls and dredging activities (Spearman et al., 1998). However, the shoal area in northern Seine Estuary (France) had decreased by 62% over the past 27 years because of the construction of several dykes, a bridge, and new port facilities (Antoine et al., 2009). Now that estuarine hydraulic engineering projects could result in both accretion and recession of estuarine shoals, it is necessary to intensify research on the response of estuarine shoals to engineering interferences.

In addition, reclamation has been widely conducted within estuaries to create more land for urban expansion (Hodoki and Murakami, 2006; Hoeksema, 2007). Although the initial accretion from reclamation projects could significantly accelerate shoal accretion, reclamation acts as the most direct contributor to shoal recession, which could roughly cut off the supratidal and upper inter-tidal zones in shoals (Yun, 2010). The Zuiderzee tidal estuary (Netherlands) was drained and reclaimed to build land during the 20th century, resulting in vast shoal degradation (Hoeksema, 2007). Similarly, the shoal area in the Ariake Bay (Japan) decreased by 16 km^2 during the early 1990s due to the Isahaya Reclamation Project (Hodoki and Murakami, 2006). However, little was known regarding the morphodynamic processes of estuarine shoals under reclamation and associated accretion promotion projects.

Despite intensive artificial interferences, accelerating sea-level rise and increasingly frequent storms from climate change increase the risk of shoal erosion and submergence, respectively (Knutson et al., 2010; Nicholls and Cazenave, 2010). Besides, various natural forcings can control trends and fluctuations in estuarine shoal morphodynamics. Shoreline changes in the Niger Estuary (Nigeria) over the last 100 years were influenced by rainfall variability and the resultant river discharge variations, which were ultimately driven by regional climate change (Dada et al., 2015). Meanwhile, water discharge is responsible for seasonal and multi-year fluctuations in estuarine morphodynamics with extremely high sediment influx and high erosion potential during the flood season and flood years, which could be found in the shoals of the Gironde Estuary (France) and Changjiang Estuary (Billy et al., 2012; Wei et al., 2016). Similarly, tides dominate the short-term deposition of estuarine shoals during calm weather to form sand-mud couplet under neap-spring cyclicity (Fan and Li, 2002). Embedded storms could result in significant sediment redistribution between estuarine shoals and channels (Yang et al., 2003; Dai et al., 2014). Additionally, both the shoal morphodynamics and related estuarine evolution could exhibit stage changes under natural and artificial forcings. For instance, the Plassac tidal bar in the Gironde Estuary indicated distinct variations in the number, size and shape-based of spits and lobes and the presence or absence of sand bodies during different stages from 1905 to 2008 (Billy et al., 2012).

Estuarine shoals worldwide are facing intensive human disturbances, so the linkage between estuarine shoal morphodynamics and different human interferences has received increasing attention. Some recent studies have been conducted on the morphodynamic processes of estuarine shoals in response to artificial engineering through field surveys and modelling, which covered scopes of hydrodynamic regime variations, sediment transport, accretion processes and geomorphic changes (Lafite and Romaña, 2001; van der Wal and Pye, 2003; Kim et al., 2006; van der Wegen et al., 2010; Rossington et al., 2011). However, it is unclear that whether and to what degree riverine loads changes induced by damming will affect estuarine shoal evolution and few studies examines how estuarine shoal morphodynamics are affected by couplings between river damming and intensive estuarine engineering projects. Besides, discerning changes from artificial interferences in river basins and within estuaries remains a formidable task.

In this study, the Nanhui Shoal (NHS) in the Changjiang Estuary was selected to diagnose recent estuarine shoal morphodynamics under the influence of dramatic engineering projects in catchments and within estuaries based on newly acquired seasonally surveyed bathymetric data during 1998–2013 and corresponding hydrological data and remote sensing images. The main aims of this study are 1) to systematically examine the NHS's recent morphodynamic processes under intensive artificial interferences; and 2) to discern the respective impacts of river damming, estuarine hydraulic engineering and reclamation on NHS morphodynamics. This work provides new insights into the response of estuarine shoals to integrated artificial interferences in river basins and estuaries.

2. Regional setting

The Changjiang Estuary is the largest estuary in the Eurasian continent (Fig. 1a), and the most populous estuary in China (Dai et al., 2014). Vast estuarine shoals (Fig. 1b), including the Chongming Shoal, Hengsha Shoal, Jiuduan Shoal and Nanhui Shoal, have developed thanks to plentiful distal suspended sediment input (larger than 400 mt/yr

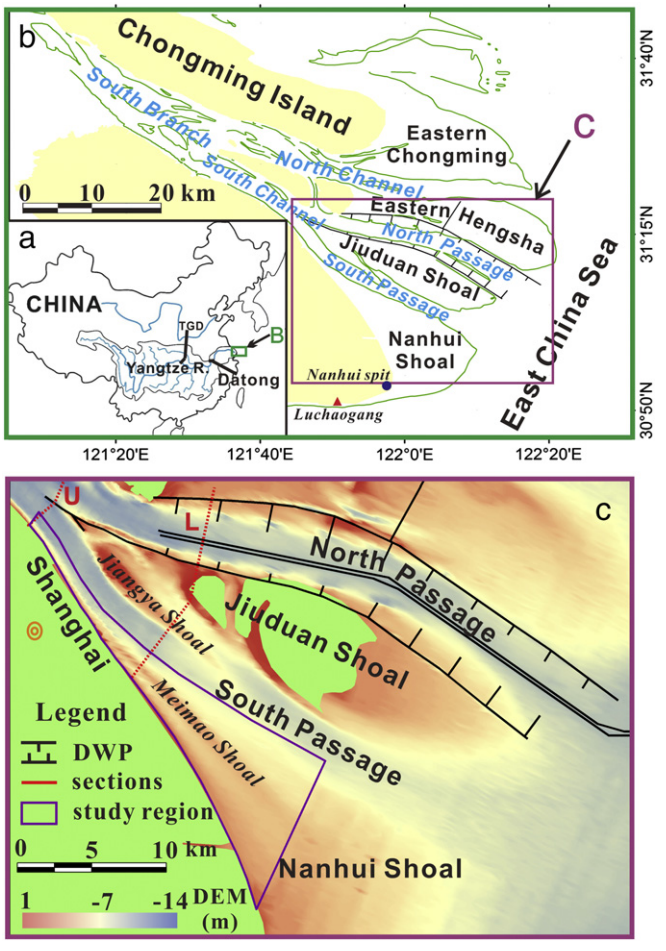

Fig. 1. Maps of a) China, which shows the drainage basin of the Changjiang River and the locations of the Three Gorges Dam and Datong station; b) geographic setting of the Changjiang estuary, including the Nanhui Shoal, South Passage, and Luchaogang gauge station; and c) landform of the Nanhui Shoal that was surveyed in 2002, which shows the locations of the Jiangya Shoal, Meimao Shoal, Deep Waterway Project, configurations of the study region, and sections for calculating the ebb flow diversion ratios.

during 1950–2000) from the Changjiang River (Chen et al., 1985). However, the recent evolution of the Changjiang estuary has suffered dramatic changes from intensive artificial interferences in catchment and within estuary (Yun, 2004). The operation of the Three Gorges Dam (TGD) in 2003 has significantly decreased Changjiang riverine sediment by 70%, and local erosion has been detected in the Changjiang Estuary (Yang et al., 2011; Dai et al., 2014). Additionally, the initiation of the Deep Waterway Project (DWP) in the North Passage during 1998–2010 (Fig. 1b), which is China's largest estuarine hydraulic engineering project, has dramatically changed the regional hydrodynamics, altering the ebb flow diversion between the North and South Passages (Hu and Ding, 2009a). Moreover, reclamation projects were widely conducted for the urban expansion of Shanghai, with 1259 km^2 of reclaimed land from 1950s to 2010 (Yun, 2010; Wei et al., 2015).

The focus of this study, the NHS, is the largest marginal shoal in the Changjiang Estuary, which plays a tremendous role in storm protection, defense against rising sea level, and land production for Shanghai (Fig. 1c). The shoal is located along the southern estuary bank, which borders the South Passage. The NHS exhibits a unique morphology, with a long-narrow tidal channel (the Meimao Trough) that lies nearly parallel to the shoreline and is separated by a tidal ridge (the Meimao Shoal) from the top of the NHS. The width of the NHS indicates a downward increasing trend from the upstream edge to the shoal's cusp, after which the trend dramatically decreases downward. Tidal, fluvial and wave processes are the main factors that control the NHS's evolution.

The NHS experiences a semidiurnal tide with a mean tidal range of 3.2 m and spring tidal range of 4 m, as gauged at Luchaogang (Fig. 1b). Besides, the tidal flow around the NHS indicates dramatic spatial variances, which exhibit bi-directional currents along the South Passage to the south of the shoal's cusp, rotating flow within the shoal's cusp, and bi-directional flow again along the southern edge (Yan et al., 2011). The present study is concentrated in the region to the north of the shoal's cusp, which is dominated by bi-directional tidal flow along the South Passage. The NHS is wave exposed, with a mean wave height of 1 m (recorded at the offshore Nanhui spit, Fig. 1b) and a wave height of approximately 6 m during stormy weather (Chen et al., 1985). Embedded extreme floods have occurred in the Changjiang Basin and Estuary, which have significantly changed the estuarine morphology and molded the present estuarine configuration of the Changjiang Estuary (Yun, 2010).

The South Passage acts as a major conduit for exporting Changjiang riverine loads (Milliman et al., 1985), so the NHS is an excellent example to explore the linkage between estuarine shoals and upstream interferences, such as a dramatic decrease in sediment input owning to operation of the TGD. Besides, recent morphodynamic processes in the NHS could have been affected by previous engineering projects, including the DWP and vast reclamation projects, because of the shoal's geographic location. However, few have been conducted to understand the couplings between the NHS and the conjugation of TGD, DWP, and reclamation projects. Considering rare catastrophic floods have occurred since 1998 (Yun, 2004), couplings between the morphodynamic processes of the NHS and artificial engineering since 1998 could exhibit how anthropogenic activities affect morphodynamic changes of the NHS without flood interferences.

3. Data and methods

3.1. Data acquisition

Our data consisted of 4 groups. The first group included bathymetric data of NHS, which were monitored by the Changjiang Estuary Waterway Administration Bureau (CJWAB), Ministry of Transportation (homepage: www.cjkhd.com). The acquired bathymetric data covered the period from 1998 to 2013 on a semi-annual basis (Table 1) and exhibited relatively high-accuracy standards (with a vertical error of 0.1 m and positioning error of 1 m) by using shipborne dual-frequency echo sounders in depth measurement and GPS devices (by Trimble, USA) in positioning. However, the data only covered partial subaerial region of the NHS because no Lidar or RTK measurements were conducted in the intertidal zone and the supratidal zone to cooperate the shipborne instrument monitoring.

Table 1
Selected bathymetric data covering NHS, Yangtze Estuary, by CJWAB.

Year	February	May	August	September	November	December	Scale
1998				√			1:25,000
1999	√		√				1:25,000
2000	√		√				1:25,000
2001	√		√				1:25,000
2002	√		√		√	√	1:25,000
2003	√		√				1:25,000
2004			√				1:10,000
2005	√		√				1:10,000
2006	√		√				1:10,000
2007	√				√		1:10,000
2008		√			√		1:10,000
2009		√			√		1:10,000
2010	√		√				1:10,000
2011	√		√				1:10,000
2012	√		√				1:10,000
2013	√		√				1:10,000

Note: Topographic campaigns are marked with '√'.

The second group included monthly water discharge and suspended sediment flux data during 1998–2013 at Datong Station (tidal limit of the Changjiang Estuary), which were acquired from the Bulletin of China River Sediment (BCRS) (available at: www.cjh.com.cn/). Specifically, multiple shipborne ADCPs (Acoustic Doppler Current Profilers) from the RD Company and ultrasonic depth transducers (or sounding weights) were used to monitor the profile velocities and depths of different subsections. Subsequently, an AMS Discharge Measurement System was introduced to compute the water discharge through the entire section. Nine samples that were distributed over 3 vertical sections were selected to conduct synchronous suspended sediment concentration measurements. The sediment flux was computed by multiplying the water discharge by the mean suspended sediment concentration of the 9 samples (Cai, 1993). The data were placed through rigorous verification and uncertainty analysis following government protocols to ensure the system-wide confidence level of above 95% (Dai and Liu, 2013).

The third group included ebb flow diversion ratios of the South Passage during 1998–2012, which were collected from the Changjiang Estuary Waterway Administration Bureau. The ebb flow diversion ratio of the South Passage was defined as the ratio of the ebb tidal volume through the selected section in the South Passage (upper section or lower section in Fig. 1c) to the sum of that through the North and South Passage, which were observed simultaneously by multiple ADCPs from the RD Company.

The fourth group included Landsat images, which were obtained from the geospatial data cloud, Computer Network Information Center, Chinese Academy of Science. Here, 4 Landsat images (Table 2) with no cloud coverage and lower tidal levels were selected.

Table 2
Selected Landsat images used for diagnosing impacts of reclamation projects on NHS's evolution.

No.	Sensor	Acquisition date	Scene center scan time
1	Landsat 7 ETM +	1999-11-03	02:17:52.4792813Z
2	Landsat 7 ETM +	2005-08-15	02:14:20.1657199Z
3	Landsat 7 ETM +	2009-01-14	02:14:41.3770313Z
4	Landsat 8 OLI	2013-08-29	02:27:03.2951292Z

3.2. Methods

The morphodynamic processes of the NHS during 1998–2013 were explored based on the bathymetric data through a series of analyses, including morphological changes, volume and area variations, and elevation frequency distribution comparisons (van der Wal and Pye, 2003; Blott et al., 2006). Raw bathymetric data were first transferred onto Beijing 54 coordinates and calibrated into 'Wusong Datum' in ArcGIS 10.1. Subsequently, data from each survey were gridded by the Kriging interpolation method into 50 m to generate a digital elevation model (DEM).

Representative DEMs of the NHS in given years were selected to analyze the morphological changes of the NHS. The −5 m isobaths of the NHS and adjacent shoals were depicted to diagnose the progradation-retreat of the NHS. Meanwhile, bathymetric changes of the NHS were produced to diagnose the spatial-temporal variations in the NHS's morphodynamic processes. Furthermore, variations in shoal volume above −5 m between surveys were extracted from the DEMs to obtain intrinsic periodic oscillation characteristics of NHS morphodynamics by using continuous wavelet transformation (Torrence and Compo, 1998). To better explore variations in the NHS's evolution at different elevations, the area of each year was calculated from the DEM by predefining a reference elevation, which represented the envelope area between the landward boundary of the study region and specific elevation isobaths, and the area variation series could quantify the isobaths' progradation-retreat with time. Generally, the shoal area in the Changjiang estuary was estimated from the bathymetry above elevation of 0 m, which was the main reclamation region. The area of the shoals was considered above an elevation of −2 m, which was correlated to the definition of shoal sub-landforms, such as tidal channels and tidal ridges, while the bathymetrical contours of −5 m was often the boundary between shoals and channels. The shoal areas above 0 m, −2 m, and −5 m were estimated to systematically evaluate variations in the NHS. The elevation frequency distribution of the NHS was also computed to explore variations in enrichment of elevation with bathymetric changes.

Here, the continuous wavelet transform could be expressed as follows (Torrence and Compo, 1998):

$$W(a,b) = \langle x(t), \varphi_{a,b}(t)\rangle = \int_{-\infty}^{+\infty} x(t)\varphi^*_{a,b}(t)dt = \frac{1}{\sqrt{a}}\int_{-\infty}^{+\infty} x(t)\varphi^*\left(\frac{t-b}{a}\right)dt \quad a, b\in R, a\neq 0 \tag{1}$$

where x(t) is the NHS's volume variations between surveys; a and t are the scale and time parameters, respectively; $\varphi(t)$ is the wavelet basis function; and $\varphi^*(t)$ is the complex conjugate of $\varphi(t)$. The complex Morlet wavelet was selected as the basis wavelet function:

$$\varphi(t) = \frac{1}{\sqrt{\pi f_b}} e^{i2\pi f_c t - (t^2/f_b)} \tag{2}$$

where f_c represents the central frequency, and f_b indicates the bandwidth.

Meanwhile, impacts of specific artificial interferences were discerned based on the last 3 groups of data. Specifically, monthly water discharge and sediment flux data were employed to detect the response of NHS evolution to the operation of the TGD, which significantly influenced the riverine load variations of the Changjiang River. Ebb flow diversion ratio data for the South Passage were used to analyze the possible effects of the DWP on NHS morphodynamics, which could alter flow bifurcations between the South Passage and the North Passage. Finally, Landsat images were introduced to diagnose the NHS evolution in relation to the reclamation projects. All the above-mentioned analyses were conducted within specific regions, as shown in Fig. 2.

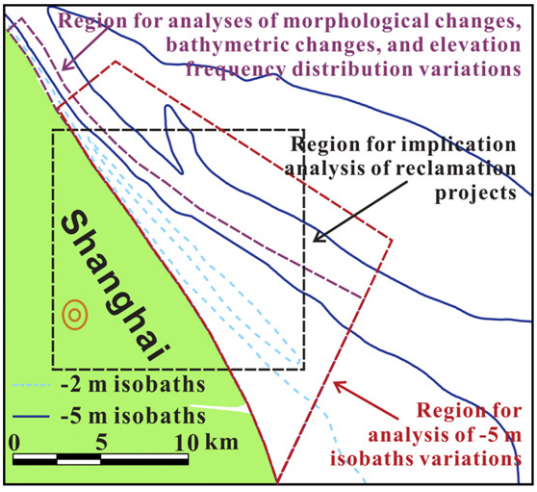

Fig. 2. Chosen regions for analyses of the morphological changes, bathymetric changes, elevation frequency distribution variations, −5 m isobaths variations and implications of reclamation projects.

4. Results

4.1. Morphological changes of the NHS

During 1998–2013, the NHS experienced geomorphic alteration with erosion along the upstream seaward edge and significant accretion in landward regions (Figs. 3–5). Besides, distinct differences existed in the shoal configuration during 1998–2013, with a long and complete tidal channel (Meimao Trough) before 12.2002, which was disrupted after 02.2003 and finally filled after 05.2009. Thus, the morphological changes of the NHS during 1998–2013 could be divided into the following 3 stages (Figs. 3–5):

Stage 1 (09.1998–12.2002) – Mild accretion with a complete tidal channel: The Meimao Trough exhibited a long and narrow configuration during 09.1998–12.2002, while the NHS was highly dynamic with an advancing-retreating seaward edge, which corresponded to the repeated downward extension and upward retreat of the Meimao Shoal (Fig. 3a–g). During 09.1998–02.1999, middle of the NHS's seaward edge gradually retreated to the downstream section, and the Meimao Shoal retreated upstream by 5 km, with the tail end separating from the upper-most shoal (Figs. 3a–b and 4a). However, middle of the NHS's seaward edge advanced northeastward by nearly 1 km during 02.1999–02.2000, with an upheaval formed in the middle section in 02.2000 (Fig. 4b). Meanwhile, the Meimao Shoal extended downward, with the tail connecting to the upper-most shoal again in 02.2000 (Fig. 3c). Subsequently, the middle of NHS's seaward edge advanced and retreated cyclically, together with cyclic extending-retreat of Meimao Shoal, with the middle of the NHS's seaward edge and the Meimao Shoal retreating during 02.2000–08.2000, 02.2001–02.2002, and 08.2002–12.2002, which was followed by the advance of the middle of the NHS's seaward edge and the downward extension of the Meimao Shoal during 08.2000–02.2001 and 02.2002–08.2002 (Fig. 3d–g). Meanwhile, the Meimao Trough cyclically opened and closed with the Meimao Shoal's evolution. Thus the NHS exhibited alternative accretion and scouring, and insignificant net bathymetric changes (0.03×10^8 m^3) during 1998–2002, experiencing slight erosion along the northern seaward edge and slight accretion in the shoals between elevation of −2 and −5 m in the south section (Figs. 3–5).

Stage 2 (02.2003–11.2008) – Filling of the disrupted tidal channel: During 2003–2008, the Meimao Trough experienced continuous infilling (Fig. 3). In 02.2003, the Meimao Trough was disrupted into 3 small pieces, among which the largest 2 acted as a long strip, while the Meimao Shoal was cracked and became connected with the upper-most shoal by −2 m isobaths in the middle (Fig. 3h). The Meimao

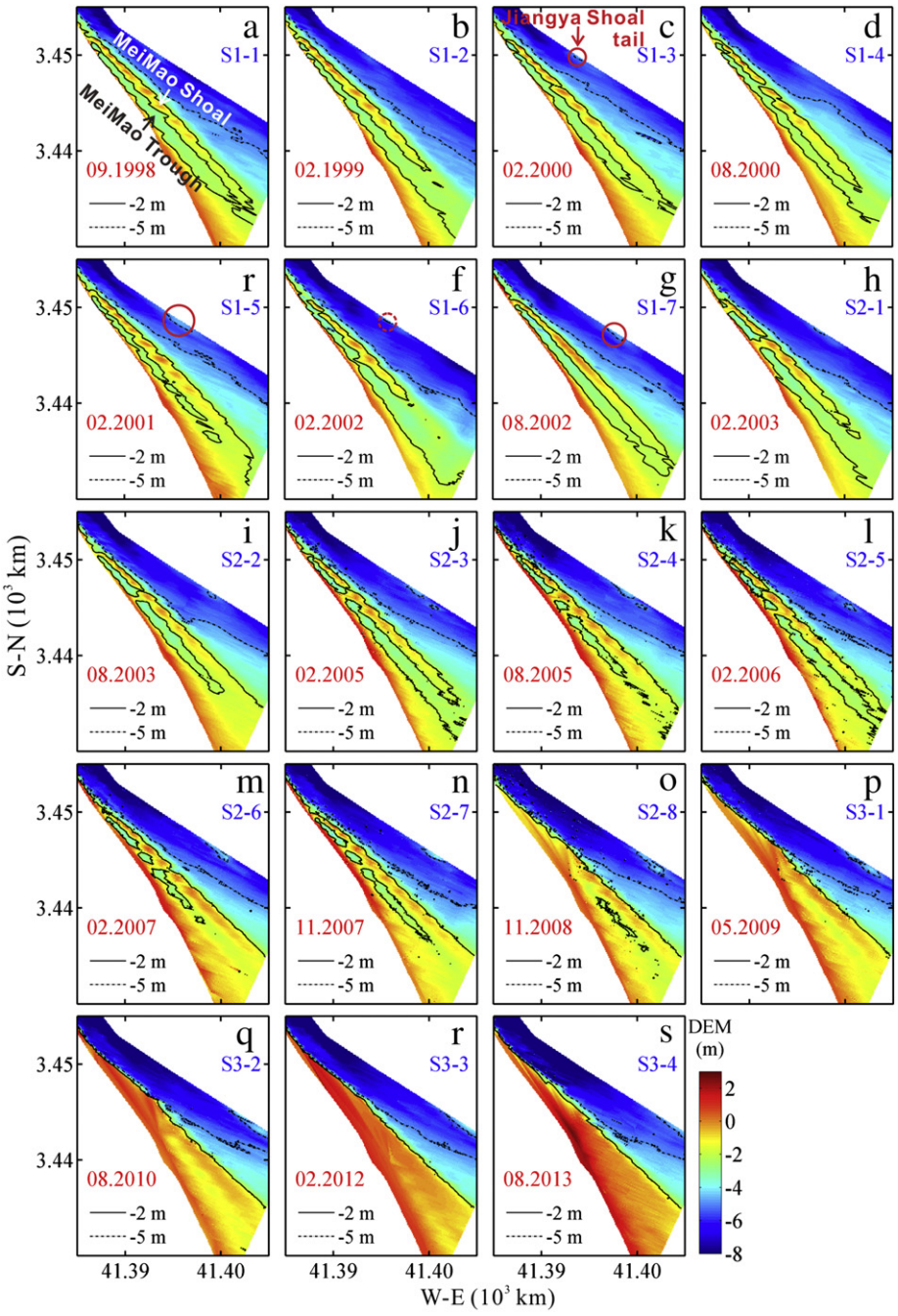

Fig. 3. Representative DEM and isobaths (−2 and −5 m) of the NHS for 3 stages, with a–g) showing Stage 1, h–o) showing Stage 2 and p–s) showing Stage 3. Obviously, the Meimao Trough had long and complete form in Stage 1, became disrupted in Stage 2 and disappeared in Stage 3. The red circle marks stretching of the Jiangya Shoal's tail within the study area during Stage 1, with the solid circle indicating the significant stretching of Jiangya Shoal's tail and the dashed circle indicating the slight stretching of the Jiangya Shoal's tail. (For interpretation of the references to color in this figure legend, the reader is referred to the web version of this article.)

Shoal extended downward again during 02.2003–08.2003, with the tail end connecting with the upper-most shoal in 08.2003, and the 2 upstream tidal channel fragments merged (Fig. 3h–i). The Meimao Shoal continued its extension-retreat cycles in 08.2003–02.2005–08.2005–02.2006, while the changing intensity grew less intense relative to that before 02.2003 (Fig. 3h–l). In this process, the main body of the Meimao Trough retained its long strip configuration and exhibited alternative closure and opening at the downward end, which was crushed into more fragments after 08.2005. Since 02.2007, the Meimao Trough has exhibited a relatively small area, which was concentrated in the upstream region in 2007 and downstream region in 2008 before finally disappearing in 2009 (Fig. 3m–p). Meanwhile, the cyclic evolution of the Meimao Shoal stopped. Relatively, the cyclic advance-retreat of the NHS's seaward edge continued during 2003–2008 but was less dramatic, similar to the Meimao Shoal's evolution. However, the cyclic evolution of the NHS's seaward edge was not synchronous to that of the Meimao Shoal, which changed in cycles of 02.2003–02.2006, 02.2006–05.2008 and after 05.2008 (Fig. 4e–g). Additionally, the regions that suffered cyclic advancing-retreat gradually migrated to the downstream region. Despite persistent erosion along the northern seaward edge, significant accretion (0.5×10^8 m^3) was detected during 2003–2008, which was concentrated in the Meimao Trough region (Fig. 5).

Stage 3 (05.2009–08.2013) - Landward accretion of the infilled tidal channel: After 05.2009, the Meimao Trough had disappeared, with the

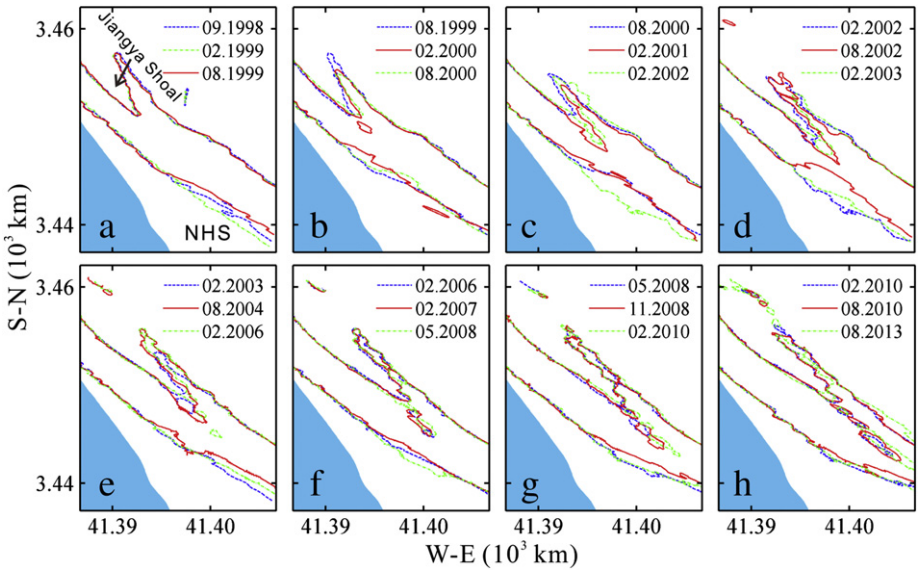

Fig. 4. −5 m isobaths of the NHS, which depict growth history of the NHS in relation to the Jiangya Shoal. Each panel corresponds to an advance-retreat cycle of NHS.

−2 m isobaths disappearing and the Meimao Shoal merging with the uppermost shoal; thus, the long-lasting tidal channel-ridge configuration had ended (Fig. 3p–s). The −2 m isobaths of NHS comprised a single straight line, which was adjacent to the −5 m isobaths in the upstream region and far from these isobaths in the downstream region (Fig. 3p–s). Meanwhile, the tail region of the former Meimao Trough was relatively low-lying, with an elevation below −1 m in 05.2009, the majority of which grew above −1 m in 08.2010 and 0 m in 02.2012 (Fig. 3q–r). Until 08.2013, the former Meimao Trough region had risen to higher than 0 m, causing the NHS to exhibit gentle and wide shoals above −2 m relative to the shoals between −2 and −5 m (Fig. 3s). Following relatively significant retreating during 11.2008–02.2010 and advancement during 02.2010–08.2010, the cyclic advance-retreat of the NHS's seaward edge stopped during 08.2010–08.2013, which indicated a gradual retreating trend (Fig. 4g–h). Generally, the period during 05.2009–08.2013 was characterized by high-paced accretion west of the Meimao Shoal, especially in the original Meimao Trough region, which experienced accretion that approached 2 m (Figs. 3p–s and 5c). The cumulative deposition volume of this stage was approximately 1×10^8 m^3 (Fig. 5d). Meanwhile, the northern seaward edge experienced erosion, and the shoals below −2 m in the southern section changed slightly.

Taken altogether, the NHS experienced dramatic bathymetric changes during 1998–2013, with a significant accretion of 1.8×10^8 m^3 west of the tidal ridge and an erosion of 0.3×10^8 m^3 east of the ridge, which indicate an overall volume increase of 1.5×10^8 m^3 (Figs. 3–5). Meanwhile, the NHS's morphodynamics during 1998–2013 indicated stage-based changes, which experienced mild accretion when the tidal channel was long and complete during 1998–2002, strong sedimentation in the disrupted tidal channel during

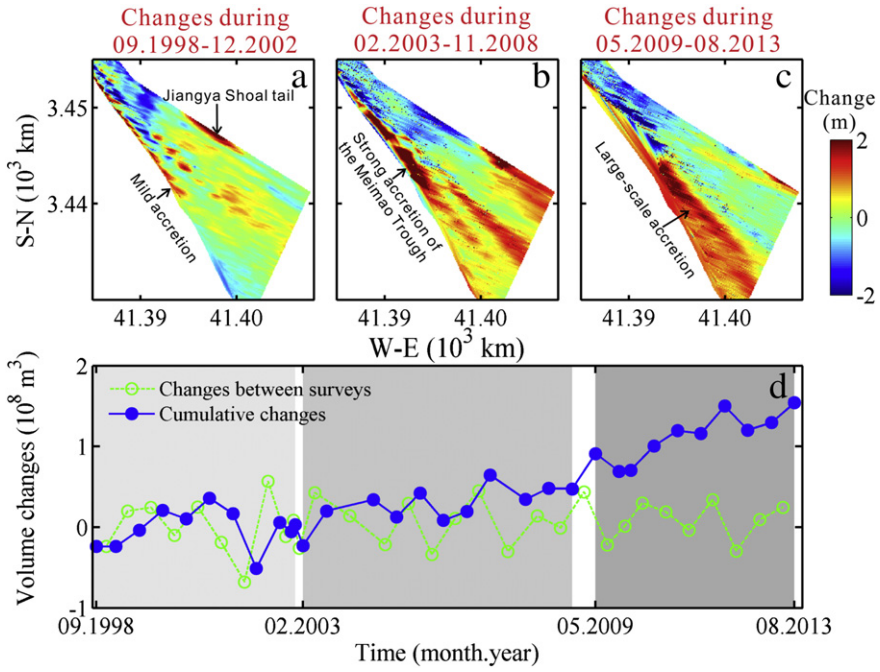

Fig. 5. a–c) Bathymetric changes of NHS during each stage, and d) temporal volume changes of NHS, with volume changes between surveys shown by dashed green line and cumulative volume changes shown by solid blue line. (For interpretation of the references to color in this figure legend, the reader is referred to the web version of this article.)

2003–2008, and large-scale accretion west of the tidal ridge after 2009, after the tidal channel was filled (Fig. 3).

4.2. Size variations of the NHS

During 1998–2013, area of the NHS (above −5 m) decreased slightly by 10 km^2, while areas above 0 and −2 m significantly increased by 45 and 35 km^2, respectively (Fig. 6; Table 3). Accordingly, the shoal area between −2 and −5 m drastically decreased by 45 km^2, which indicated that the shoal's transverse slope between elevation of −2 and −5 m became steep during the observed period. The area variations of the NHS during different stages were different because of the stage-based morphology (Fig. 6). The areas above 0 m and −2 m changed slightly during 09.1998–12.2002 at rates of −0.02 and 0.57 km^2/yr, respectively. During 02.2003–11.2008, the area above −2 m significantly increased at a rate of 5.19 km^2/yr, while the area above 0 m slightly increased. The rapid increase in area above −2 m stopped after 05.2009, which turned to stay stable, while area above 0 m dramatically increased at a rate of 7.71 km^2/yr. Relatively, the area above −5 m kept decreasing at an accelerating rate during 1998–2013 (Fig. 6c).

Fluctuations could also be detected in the area variations above −2 m before 02.2006 and above −5 m before 08.2010 (Fig. 6). Specifically, the area above −2 m exhibited irregular fluctuations during 09.1998–12.2002 and rose in undulation during 02.2003–02.2006. Fluctuations in the area changes above −5 m were extremely significant before 02.2003, indicating a similar variation mode to that above −2 m, which became less intense during 02.2003–08.2010. Besides, the fluctuations in the areas above −2 m and −5 m were in accordance with cyclic evolution of the Meimao Shoal and the NHS's seaward edge, respectively (Figs. 3–4).

Moreover, wavelet analysis was conducted on the volume variations between surveys (Fig. 7). The shadow area within the dotted line indicated periodic components of 12–44 months, at a 95% confidence level (Fig. 7a). Furthermore, the global wavelet diagram demonstrated a significant cycle of approximately 18 months through red noise examination at a significance level of 0.05 (Fig. 7b). Fluctuations in the NHS's volume were clearly shown by the period component (18 months) extracted from the wavelet variance diagram (Fig. 7c).

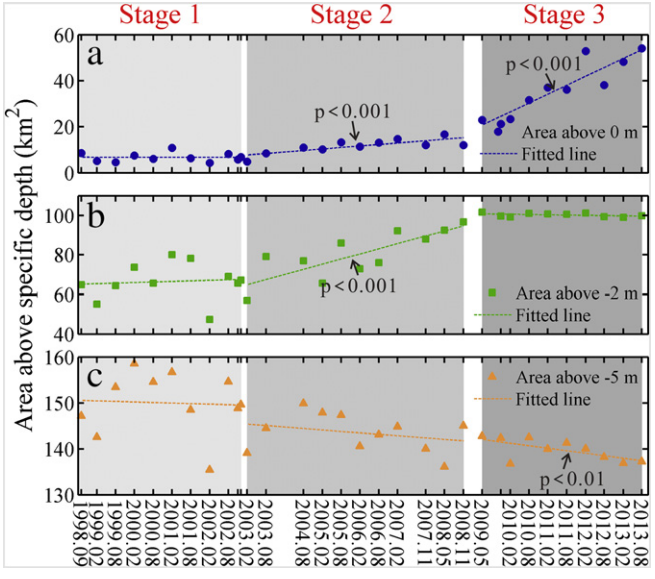

Fig. 6. Area changes of NHS a) above 0 m, b) above −2 m and c) above −5 m. The three stages are depicted by gradually deepening color areas, with the fitting line shown. (For interpretation of the references to color in this figure legend, the reader is referred to the web version of this article.)

Table 3
Area changing rate of NHS in different stages.

Stages	Stage 1	Stage 2	Stage 3	Who period
Above 0 m (km^2/yr)	−0.02	1.31	7.71	3.05
Above −2 m (km^2/yr)	0.57	5.19	−0.27	2.35
Above −5 m (km^2/yr)	−0.24	−0.64	−1.08	−0.67

Note 1: Area changing rate for each stage is gained by linear fitting, as shown in Fig. 2.
Note 2: Area changing rate for the entire period is gained through dividing change of area during the whole period by time spent.

4.3. Changes in the elevation frequency distribution

The elevation frequency distribution of the NHS suffered significant changes following the NHS's morphodynamic development. The mean elevation frequency distribution of Stage 1 (1998–2002) exhibited three major peaks, indicating 3 enriched centers of shoal elevation (Fig. 8a). The crest around −2 m was highest because of the long and wandering −2 m isobaths of NHS during this stage (Figs. 3 and 8). The wide crest around −5 m, together with a small peak around −4 m, indicated a relatively gentle slope between −4 and −6 m. The crest around −9.5 m fraction, which corresponded to the enriched elevation of South Passage, was not that developed in Stage 1.

The mean elevation frequency distribution of Stage 2 (2003–2008) covered a larger range because of accretion on shoals and erosion of the passage (Fig. 8b). Due to continuous accretion of the Meimao Trough in Stage 2, the crest around −2 m moved to higher fraction slightly, which became lower and wider simultaneously, while the crest around −5.5 m grew thinner with the previous peak around −4 m becoming less pronounced. The previous crest around −9.5 m migrated to a lower fraction and became more obvious due to deepening of the South Passage in the upstream section (Fig. 5b).

Relatively, the mean elevation frequency distribution of Stage 3 (2009–2013) covered the largest fraction range (Fig. 8c). The highest crest moved to approximately 0 m and grew significantly wider due to accretion in the region to the west of the Meimao Shoal (Figs. 5 and 8). The previous crest around −9.5 m moved to lower fraction of approximately −10.5 m, while the location of the crest at −5.5 m barely changed and the small peak around −4 m nearly disappeared. Besides, the extreme low frequency in fraction between −3 and −2 m indicated that flat between −2 and −3 m rarely developed during this stage. This results matched decrease in area between −2 and −5 m and strongly implied that a steep slope formed between −2 and −3 m after 2009 (Fig. 6).

4.4. Artificial engineering of catchment and around NHS

Multiple large-scale engineering projects were conducted in the Changjiang Basin and Estuary, including the TGD, DWP and reclamation projects. These engineering projects brought in significant changes in the Changjiang riverine loads and the regional hydrodynamics around NHS.

Despite relatively wet years in 1998 and 1999, the water discharge from the Changjiang River presented insignificant decreasing trend even after the operation of the TGD in 2003 (Mei et al., 2016). Besides, the annual water discharge cycle continued at a relatively high extent, with the flood discharge being more than 3.5 times the drought discharge (Fig. 9a). Relatively, sediment flux from the Changjiang River had sharply decreased since the TGD's initiation, with the monthly peak sediment flux decreasing from around 100 mt/month before 2003 to 60 mt/month during 2003–2005 and less than 40 mt/month after 2006 (Fig. 9b).

The DWP could alter bifurcated configuration of the North and South Passages, dramatically changing the ebb flow diversion ratio between the two passages (Hu and Ding, 2009a). As shown in Fig. 10a, the ebb flow diversion ratio of the South Passage increased from lower than

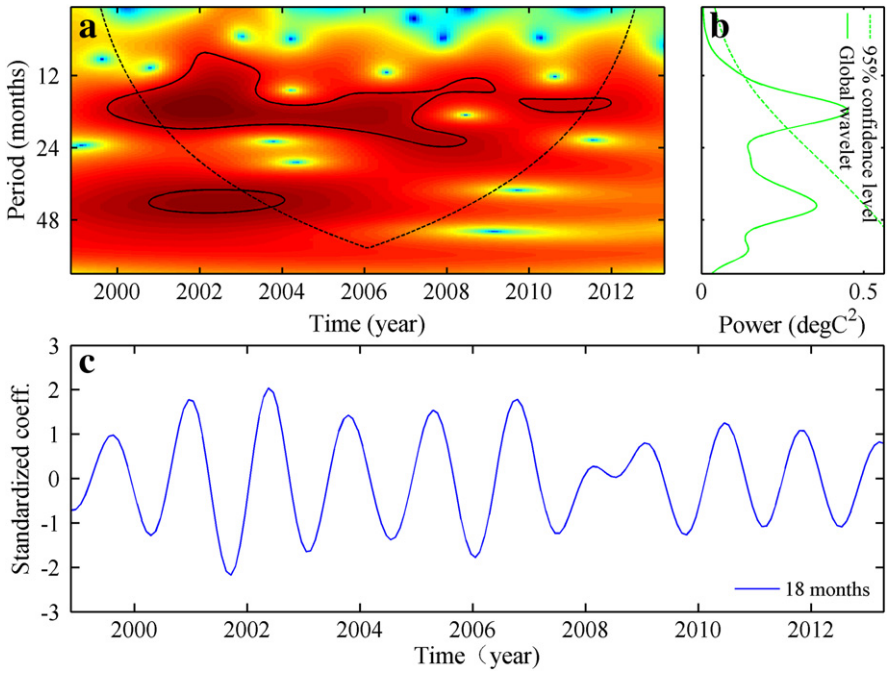

Fig. 7. Wavelet analysis of the NHS's volume changes between surveys: (a) contoured coefficient, (b) global wavelet coefficient, and (c) time series of the periodic component (namely 18 months) extracted from (a).

40% in 1999 to larger than 60% after 2009 in the upper section. Relatively, the ebb flow diversion ratio in the lower section increased to a lower extent (Fig. 10a). Thus, the ebb flow diversion ratio tended to increase less significantly in more downstream regions.

Moreover, large-scale reclamation projects, including initial accretion promotion projects, were conducted in the NHS. In terms of groin construction, accretion promotion projects were confined to the upstream region in 1999 but were extended to the downstream region by 2005 (Fig. 11a–b). Dramatic reclamation was conducted in 2009, with the land border significantly advancing seaward to the reference line (Fig. 11c). Additionally, groins that extended seaward could be seen in the upstream region in 2009, indicating additional accretion promotion projects in this region during 2005–2009. The region within the additional accretion promotion projects experienced reclamation in 2013, which had intruded into the former Meimao Trough region (Fig. 11d).

5. Discussion

5.1. Impacts of the upstream shoal stretching

The southern dike of the DWP resulted in bifurcated ebb flow along the Jiangya Shoal and induced the progradation of the Jiangya Shoal into the South Passage (Fig. 4) (Chen et al., 2011), which would have altered the regional flow mode of the South Passage and affected morphodynamics of the NHS's seaward edge. Since 02.2000, the Jiangya Shoal had stretched into South Passage in a cyclic manner, which stretched significantly within a short period and stayed relatively stable thereafter (Fig. 4). In this process, the cyclic evolution of the NHS's seaward edge and the fluctuations in area above −5 m correlated well to the phased stretching of the Jiangya Shoal. In each cycle during 08.1999–08.2010, the NHS's seaward edge tended to advance significantly as the Jiangya Shoal abruptly stretched, but then retreated with the relative stabilization of the Jiangya Shoal (Fig. 4). The Meimao Shoal showed a similar evolution mode during 08.1999–08.2002 (Fig. 3).

Cyclic hydrodynamic variations near the NHS's seaward edge from the stretching of the Jiangya Shoal could explain this phenomenon.

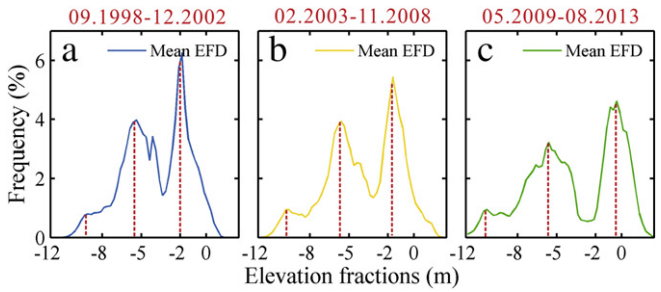

Fig. 8. a–c) Mean elevation frequency distribution (EFD) of the NHS in each stage.

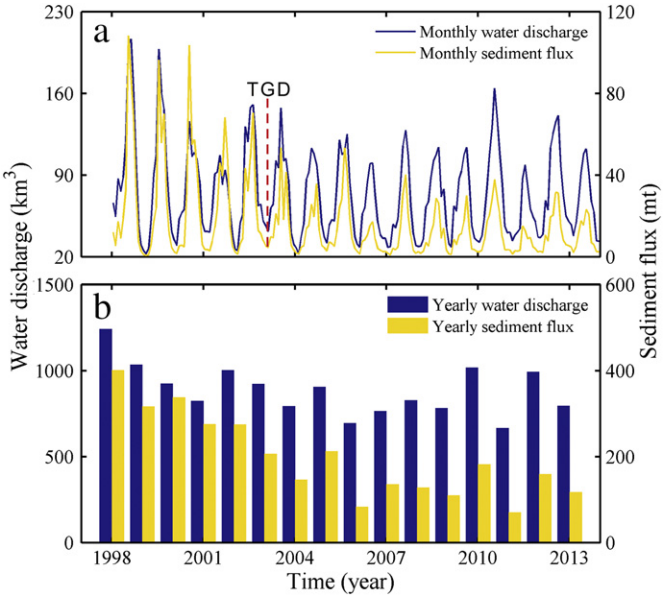

Fig. 9. a) Monthly water discharge and sediment flux and b) yearly water discharge and sediment flux from the Changjiang River, as monitored at the Datong station.

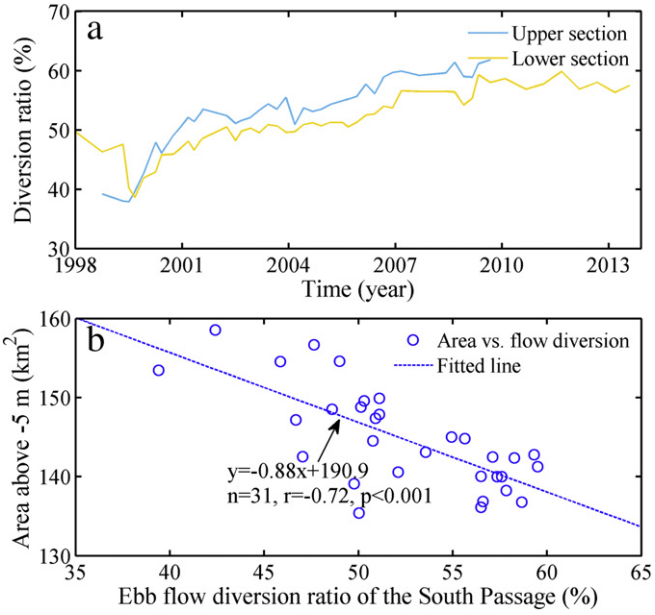

Fig. 10. a) Changes in the ebb flow diversion ratio of the South Passage through the upper and lower sections, and b) correlation between the ebb flow diversion ratio of the South Passage and the area changes of NHS above −5 m during 09.1998–08.2013.

The rapid stretching of the Jiangya Shoal indicated significant additional input to the South Passage and NHS, which could trigger the downstream extension of the Meimao Shoal and seaward advance of the NHS's seaward edge (Fig. 12b). After the significant expansion of the NHS's seaward edge with rapid stretching of the Jiangya Shoal, the smaller width between the NHS and Jiangya Shoal produced regionally intensified flow, which resulted in the seaward retreat of NHS back to the original state (Fig. 12a and c). Meanwhile, intensified rotating flow cut off the Meimao Shoal, resulting in the upward retreat of the Meimao Shoal.

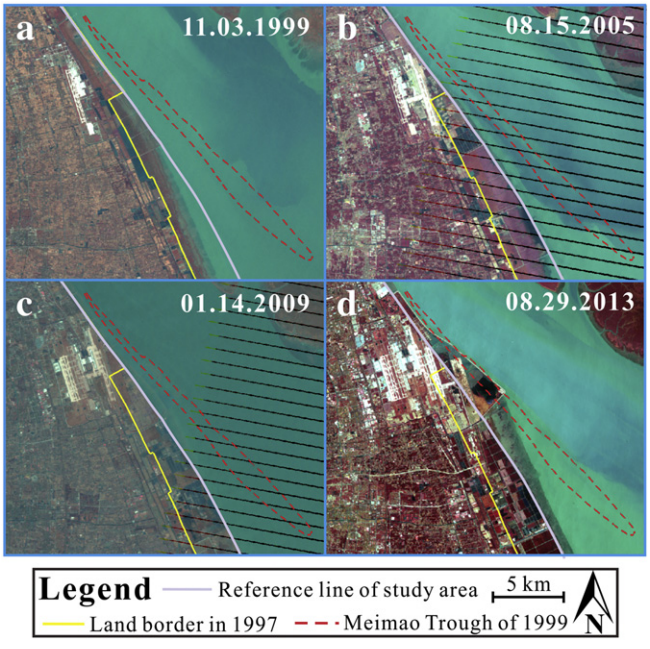

Fig. 11. Landsat images that show reclamation projects of NHS during 1998–2013.

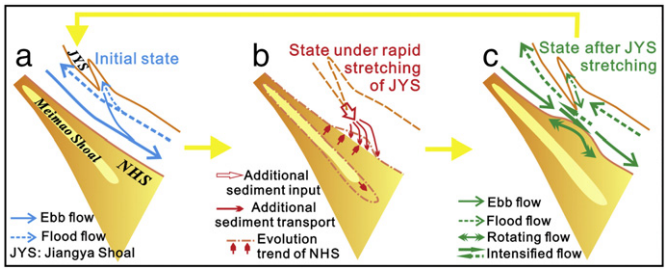

Fig. 12. Sketch that shows cyclic evolution of the NHS relative to the Jiangya Shoal's stretching, with a) the initial state, b) the state under the rapid stretching of Jiangya Shoal, and c) the state after the Jiangya Shoal's stretching.

The additional input from the rapid stretching of the Jiangya Shoal could have only affected the region near the Jiangya Shoal's tail in the NHS, so the cyclic evolution of the NHS's seaward edge became indistinctive within the study region after 08.2010, when the Jiangya Shoal's tail had migrated to the downward region. Meanwhile, the cyclic evolution of the Meimao Shoal relative to the Jiangya Shoal had been disturbed because of the continuous accretion of the Meimao Trough since 2003. After 02.2007, when the Meimao Trough was almost filled, the cyclic evolution of the Meimao Shoal was negligible. Moreover, the additional sediment transport was along longitude direction of Jiangya Shoal. When the Jiangya Shoal's tail migrated downward, the direction of the additional transport rotated anticlockwise, with the cross-shore additional transport component gradually decreasing. This explained why the intensities of the cyclic advance-retreat of the NHS's seaward edge and extension-retreat of the Meimao Shoal decreased after 02.2003.

5.2. Impacts of river damming

The almost unchanged water discharge in recent years could not explain the trend variations in the area and gradual accretion of the NHS during 1998–2013. However, the water discharge could be likely a key factor controlling periodic characteristics of the NHS's volume changes, which exhibited a cyclic fluctuation of 18 months (Figs. 7 and 13). Specifically, the volume changes tended to lag 15 months behind the water discharge (Fig. 13). The water discharge also dominated the periodic characteristics of the Jiuduan Shoal in the Changjiang Estuary, during 1998–2014, whose area presented different fluctuation modes due to different engineering interferences (Wei et al., 2016). Similarly, a ca. 25-year periodicity in both the fluvial discharge and the tidal bar's width, length and volume variations were evidenced in the Gironde estuarine tidal bar (Billy et al., 2012).

Meanwhile, although the distal sediment input significantly decreased due to the TGD's operation since 2003, the NHS experienced a cumulative accretion of approximately 1.5×10^8 m^3 (Figs. 5 and 9). Thus distal sediment input played a limited role in the NHS's morphodynamic changes considering the almost unchanged suspended sediment concentration in the turbidity maximum zone of estuary (Dai et al., 2012). The Changjiang estuarine shoal was not the only region to experience significant accretion under dramatically decreased distal sediment input from human activities in catchments. For instance, the accretion rate for the Keum Estuary in Korea actually increased after dam construction in the upper reaches, which transformed the main estuarine channel from an ebb-dominated mode to a flood-dominated one (Kim et al., 2006). Despite sharply decreased riverine loads due to upstream barrier, the accretion of the Brisbane Estuary in Australia increased because of reduced freshwater flow and continuous marine sediment input (Eyre et al., 1998). Thus, the impacts of distal sediment input on estuarine morphodynamic changes could be hindered by significantly altered estuarine sediment trapping capacity and additional available sediment source.

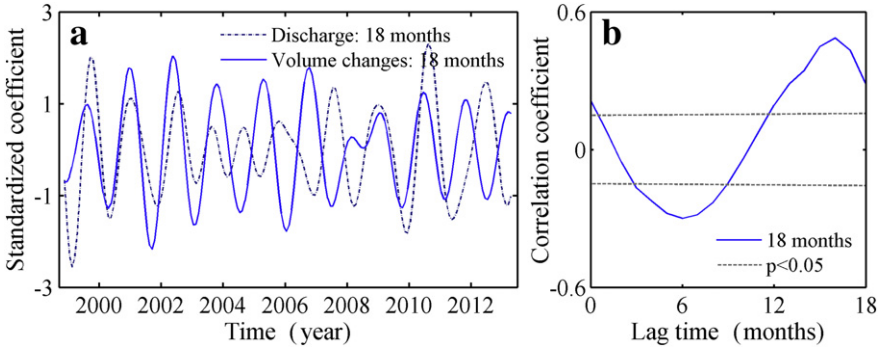

Fig. 13. Relationships between the water discharge and volume change of NHS: a) extracted periodic components of 18 months from the wavelet contoured coefficient, similar to that in Fig. 6; and b) lag correlation between the periodic components of water discharge and volume changes of NHS between surveys.

5.3. Impacts of estuarine hydraulic engineering

Since the flow within the study region mainly acted as a bi-directional current along the South Passage, the flow dynamics around the NHS stemmed from the gambling of fluvial intensity and tidal forcing. With almost unchanged water discharge from the Changjiang River (Fig. 9) and relatively stable tidal range of Changjiang Estuary after 2000 (Jiang et al., 2012), increasing ebb flow diversion ratio indicated intensified ebb flow and residual transport in the upper South Passage (Dai et al., 2015). The DWP increased the ebb flow intensity in the South Passage, which could contribute to the retreat of NHS and was well verified by the high correlation between the ebb flow diversion ratio of South Passage and the area of NHS above −5 m (Figs. 4, 6 and 10b). Considering relatively weak growth in ebb flow diversion ratio of the lower section to the upper section (Fig. 10a), the increased ebb flow diversion ratio could have only affected limited region in the upper South Passage. Thus retreat of NHS was more significant in the upward region (Figs. 4 and 5).

Although the neap-spring cyclicity of tides could induce fluctuations in the short-term deposition of estuarine shoals during calm weather, the sedimentary record could be destroyed by reworking and erosion from flows and waves during rough weather (Fan and Li, 2002). Meanwhile, significant sediment redistribution within estuaries because of storms could recover after several weeks at most (Yang et al., 2003). The NHS's evolution during 1998–2013 could exhibit neap-spring-tide and storm-recovery cycles (days to weeks) from tides and storms, which were not the focus of this present study because of variations in the time scale. Moreover, waves during stormy weather are significantly attenuated by the estuarine shoals at the Changjiang Estuary's entrance (Hu and Ding, 2009b). Thus, the studied region around the NHS was located landward of the estuary's entrance, which is barely affected by extremely high waves during storms. Nevertheless, the impacts of storm surges on NHS morphodynamics require more detailed research.

5.4. Impacts of reclamation projects

The groins that were constructed in reclamation projects could weaken regional flow intensity (Yun, 2010) and induce shoal accretion (Fig. 11). In 1999, relatively vast shoals emerged above water outside the land border of 1997, whose width decreased downward from the project region (Fig. 11a). In 2005, more shoals emerged above water as the accretion promotion projects expanded downstream (Fig. 11b). In 2009, slight newborn flats emerged within the former accretion promotion project region (Fig. 11c). In 2013, more shoals emerged in the additional accretion promotion project region, while fewer shoals emerged in the downstream region, where no extended groins were constructed (Fig. 11d). Generally, shoals within the accretion promotion region tended to emerge above water first. The research region in this study was located northward of the reference line, where vast shoals emerged during 2009–2013, just the time when flats above 0 m experienced significant accretion and the area above 0 m abruptly increased. Meanwhile, these accretion promotion constructions could also play a tremendous role in the accretion of the Meimao Trough, with subaqueous groins intruding into the previous Meimao Trough region (Fig. 11c), which was an important morphodynamic process in the NHS's evolution history (Figs. 3 and 7). In this study, the dramatic increase in area above −2 m was followed by that above 0 m, which correlated to accretion processes in the Meimao Trough region that were induced by reclamation projects.

5.5. Evolution mode of the NHS and possible implications

During 1998–2013, the NHS had suffered significant changes from multiple artificial engineering projects, and exhibited complex spatial variations in its evolutionary trends and cyclic changes (Fig. 14a and b). Despite the gradual retreat at the seaward edge, an integral siltation of 1.5×10^8 m^3 could be detected between 2003 and 2013 with the filling of the Meimao Trough during 2003–2009 and the subsequent large-scale accretion in region to the west of the Meimao Shoal after 2009 (Fig. 14). In this process, the long-lasting tidal channel-ridge structure of the NHS was destroyed, which turned to present a relatively flat top above −2 m, followed by an extremely steep slope between −2 and −3 m. Meanwhile, the relatively flat zone, indicated by a small peak around −4 m in the elevation frequency distribution in Stage 1, suffered embezzlement from the continuously retreating −5 m isobaths of NHS, and disappeared gradually. The morphodynamic changes of NHS during 1998–2013 exhibited fluctuated characteristics, with volume variations indicating an approximate 18-month period (Figs. 7 and 14). Specifically, the Meimao Shoal cyclically extended and retreated during 1998–2006, and the NHS's seaward edge cyclically advanced and retreated during 1998–2010 (Figs. 3, 4 and 14).

Multiple artificial interferences influenced the NHS morphodynamics (Fig. 14a). Generally, river damming tended to induce a decline in riverine sediment, sediment starvation and the subsequent erosion of estuarine shoals, which could be observed in the Mississippi and Mekong Estuaries (Blum and Roberts, 2009). Meanwhile, damming could trigger shoal accretion by decreasing the fluvial intensity and altering the estuarine hydrodynamics (Kim et al., 2006; Anthony et al., 2015). For the NHS, which experienced unexpected accretion during 1998–2013, it was determined that dramatic decline in distal sediment induced by damming (TGD) could play minor role in flat changes of NHS, considering the slightly changed suspended sediment concentration within the turbidity maximum zone (Dai et al., 2012), which was favored by eroded sediment from the inner estuary and outer sea (Dai et al., 2014; Luan et al., 2016). Besides, changes in the Changjiang Estuary's fluvial intensity were deemed to be limited in view of the long distance from TGD to the estuary and the stable water discharge at Datong even after 2003 (Fig. 9). Recent morphodynamic changes of NHS were more likely hydrodynamic-dominated processes that were

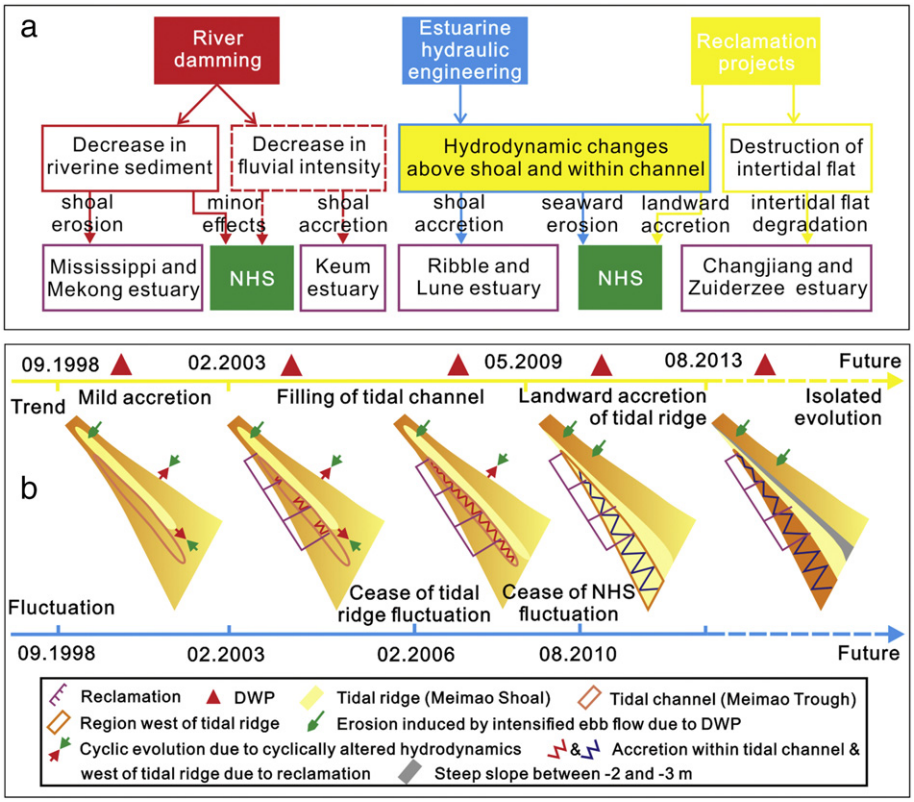

Fig. 14. a) Conceptual model depicting linkage between specific artificial engineering projects and morphodynamics of NHS and other estuarine shoals, and b) timeline of the NHS's evolution.

controlled by proximal engineering projects, including estuarine hydraulic engineering (DWP) and reclamation projects, which controlled seaward erosion by intensifying the ebb flow of the South Passage and landward accretion by promotion effects, respectively (Figs. 10, 11 and 14). Similarly, hydraulic engineering projects, such as construction and dredging were key factors that contributed to shoal accretion, including the infilling of the Ribble and Lune Estuaries, by decreasing regional the tidal flow or total tidal prism (Spearman et al., 1998; van der Wal et al., 2002). The multiple influences on the NHS suggested that the distance from a given engineering project, rather than the magnitude, might directly determine the degree of impacts on estuarine shoal evolution, especially in small estuaries and specific shoals in large estuaries worldwide.

Despite the polarized evolution modes, fluctuations were detected in NHS morphodynamics from both the fluctuating Changjiang water discharge and cyclically altered hydrodynamics of the South Passage (Figs. 12–14). Analogous cyclic evolution (both seasonal and multi-year) of estuarine shoals from water discharge could also be detected in the Jiuduan Shoal in the Changjiang Estuary and the Plassac tidal bar in the Gironde Estuary (Billy et al., 2012; Wei et al., 2016). Although complex channel-shoal interactions within estuaries were general (Hibma et al., 2003; Dam et al., 2016), the cyclically changed hydrodynamics of the South Passage from the stretching of the Jiangya Shoal (Fig. 12), ultimately the couplings of the DWP and estuarine hydrodynamics, seemed to be rare around world. Besides, NHS morphodynamics exhibited stage-based changes in terms of the configuration of the tidal channel, which resulted from the reclamation induced tidal channel filling (Figs. 3, 11 and 14). Similarly, human activities in the basin and estuary led to a stage-based evolution in the Mersey Estuary and San Pablo Bay (Thomas et al., 2002; Blott et al., 2006; Jaffe et al., 2007). Estuarine shoals could also exhibit stage-based changes under natural forcings such as fluvial and tidal controls, for instance, in the Gironde and Western Scheldt Estuaries (Billy et al., 2012; Dam et al., 2016).

The basic objective of the reclamation project was achieved, with areas above 0 m and −2 m increasing by 45 and 35 km^2, respectively (Figs. 6 and 11). However, the project was accomplished by excessively consuming future interests, because the NHS's seaward edge retreated under intensified ebb flow from the DWP, which would continue until an equilibrium was reached (Fig. 14). The flat above 0 m could continue advancing seaward as additional reclamation projects are conducted, and more new-born land could be reclaimed. However, subsequent reclamation could be significantly restricted by the steep slope that formed between −2 and −3 m (Figs. 8 and 14). Besides, the steep slope increased risk of recession in the NHS due to sea-level rise and more frequent storms (Knutson et al., 2010; Nicholls and Cazenave, 2010). Case of NHS could enlighten the exploitation of other estuarine shoals, where intensive estuarine engineering, such as reclamation projects, could effectively accelerate shoal accretion by altering the regional hydrodynamics, while the steep slope that formed from these engineering projects could increase the instability of shoals and increase the risk of shoal recession under a combination of rising sea levels and artificial engineering projects, especially for reclamation.

6. Conclusions

Intensive human activities during the anthropogenic era, have significantly altered estuarine environments with serious interferences in estuarine shoal morphodynamics. The NHS, in the Changjiang estuary, indicated a polarized evolution mode with a dramatic accretion landward from the tidal ridge and an erosion at the seaward edge during 1998–2013, under couplings of the DWP and reclamation projects. Relatively, the drastic decline in suspended sediment owning to the TGD played a minor role in the flat changes of NHS. The case of NHS indicated

that impacts of river damming on estuarine shoal could be hindered by intensive estuarine engineering, and should be analyzed dialectically considering the predominant role of damming induced decline in distal sediment or fluvial intensity.

The estuarine shoal morphodynamics could exhibit cyclic variations owing to fluctuating water discharge and cyclically altered hydrodynamics of lateral channel, such as the NHS, which showed 18-month cyclic variations. Multiple estuarine interferences could create steep slopes along estuarine shoals, which was demonstrated with an exemplar mega-estuary, namely, Changjiang estuary. This phenomenon would increase the instability of shoals and thus induce the risk of shoal recession under the combinative threat of rising sea levels and artificial engineering projects.

Acknowledgements

This study was supported by the funds from the National Natural Science Foundation of China (NSFC) (41576087), the Guangxi Natural Science Foundation (2015GXNSFBA139207), the 2015 key program of the social science and humanity of the Guangxi colleges and universities (KY2015ZD133), and the SKLEC Fostering Project for Top Doctoral Dissertations. The authors are grateful to Prof. Edward Anthony and the two anonymous reviewers for their constructive comments and suggestions.

References

Anthony, E.J., Marriner, N., Morhange, C., 2014. Human influence and the changing geomorphology of Mediterranean deltas and coasts over the last 6000 years: from progradation to destruction phase? Earth Sci. Rev. 139, 336–361.
Anthony, E.J., Brunier, G., Besset, M., Goichot, M., Dussouillez, P., Nguyen, V.L., 2015. Linking rapid erosion of the Mekong River delta to human activities. Sci. Rep. 5 (14745), 1–12.
Antoine, C., Julien, D., Robert, L., Christophe, B., 2009. Morphological responses of an estuarine intertidal mudflat to constructions since 1978 to 2005: the Seine estuary (France). Geomorphology 104, 165–174.
Billy, J., Chaumillon, E., Féniès, H., Poirier, C., 2012. Tidal and fluvial controls on the morphological evolution of a lobate estuarine tidal bar: the Plassac Tidal Bar in the Gironde Estuary (France). Geomorphology 169–170, 86–97.
Blott, S.J., Pye, K., van der Wal, D., Neal, A., 2006. Long-term morphological change and its causes in the Mersey Estuary, NW England. Geomorphology 81 (1–2), 185–206.
Blum, M.D., Roberts, H.H., 2009. Drowning of the Mississippi Delta due to insufficient sediment supply and global sea-level rise. Nat. Geosci. 2, 488–491.
Cai, K.J., 1993. Flow measurement in large rivers in China. Flow Meas. Instrum. 4 (1), 47–50.
Chen, J.Y., Zhu, H.F., Dong, Y.F., Sun, J.M., 1985. Development of the Changjiang estuary and its submerged delta. Cont. Shelf Res. 4 (1/2), 47–56.
Chen, W., Li, J.F., Jiang, C.J., 2011. Characteristics of recent morphological evolution of Jiuduansha Shoal in Yangtze Estuary. J. Sediment. Res. 1, 15–21.
Dada, O.A., Qiao, L.L., Ding, D., Li, G.X., Ma, Y.Y., Wang, L.M., 2015. Evolutionary trends of the Niger Delta shoreline during the last 100 years: responses to rainfall and river discharge. Mar. Geol. 367, 202–211.
Dai, Z.J., Liu, J.T., 2013. Impacts of large dams on downstream fluvial sedimentation: an example of the Three Gorges Dam (TGD) on the Changjiang (Yangtze River). J. Hydrol. 480, 10–18.
Dai, Z.J., Chu, A., Li, W.H., Li, J.F., Wu, H.L., 2012. Has suspended sediment concentration near the mouth bar of the Yangtze (Changjiang) Estuary been declining in recent years? J. Coast. Res. 29 (4), 809–818.
Dai, Z.J., Liu, J.T., Fu, G., Xie, H.L., 2013. A thirteen-year record of bathymetric changes in the north passage, Changjiang (Yangtze) Estuary. Geomorphology 187, 101–107.
Dai, Z.J., Liu, J.T., Wei, W., Chen, J., 2014. Detection of the Three Gorges Dam influence on the Changjiang (Yangtze River) submerged delta. Sci. Rep. 4 (6600), 1–7.
Dai, Z.J., Liu, J.T., Wen, W., 2015. Morphological evolution of the South Passage in the Changjiang (Yangtze River) estuary, China. Quat. Int. 187, 101–107.
Dam, G., van der Wegen, M., Labeur, R.J., 2016. Modeling centuries of estuarine morphodynamics in the Western Scheldt estuary. Geophys. Res. Lett. 43 (8), 3839–3847.
Dyer, K.R., Christie, M.C., Wright, E.W., 2000. The classification of intertidal mudflats. Cont. Shelf Res. 20, 1039–1060.
Eyre, B., Hossain, S., McKee, L., 1998. A suspended sediment budget for the modified subtropical Brisbane River Estuary, Australia. Estuar. Coast. Shelf Sci. 47, 513–522.
Fan, D.D., Li, C.X., 2002. Rhythmic deposition on mudflats in the meso-tidal Changjiang estuary, China. J. Sediment. Res. 72 (4), 543–551.
Hibma, A., de Vriend, H.J., Stive, M.J.F., 2003. Numerical modelling of shoal pattern formation in well-mixed elongated estuaries. Estuar. Coast. Shelf Sci. 57, 981–991.
Hodoki, Y., Murakami, T., 2006. Effects of tidal flat reclamation on sediment quality and hypoxia in Isahaya Bay. Aquat. Conserv. Mar. Freshwat. Ecosyst. 16 (6), 555–567.
Hoeksema, R.J., 2007. Three stages in the history of land reclamation in the Netherlands. Irrig. Drain. 56, S113–S126.
Hu, K.L., Ding, P.X., 2009a. The effect of deep waterway constructions on hydrodynamics and salinities in Yangtze estuary, China. J. Coast. Res. SI56, 961–965.
Hu, K., Ding, P.X., 2009b. A 2D/3D hydrodynamic and sediment transport model for the Yangtze Estuary, China. J. Mar. Syst. 77 (1–2), 114–136.
Jaffe, B.E., Smith, R.E., Foxgrover, A.C., 2007. Anthropogenic influence on sedimentation and intertidal mudflat change in San Pablo Bay, California: 1856–1983. Estuar. Coast. Shelf Sci. 73, 175–187.
Jiang, C.J., Li, J.F., de Swart, H.E., 2012. Effects of navigational works on morphological changes in the bar area of the Yangtze estuary. Geomorphology 139-140, 205–219.
Kim, S.G., 2010. The evolution of coastal wetland policy in developed countries and Korea. Ocean Coast. Manag. 53, 562–569.
Kim, T.I., Choi, B.H., Lee, S.W., 2006. Hydrodynamics and sedimentation induced by large-scale coastal developments in the Keum River Estuary, Korea. Estuar. Coast. Shelf Sci. 68 (3–4), 515–528.
Knutson, T.R., McBride, J.L., Chan, J., Emanuel, K., Holland, G., Landsea, C., Held, I., Kossin, J.P., Srivastava, A.K., Sugi, M., 2010. Tropical cyclones and climate change. Nat. Geosci. 3, 157–163.
Lafite, R., Romaña, J.L., 2001. A man-altered macrotidal estuary: the Seine estuary: introduction to the special issue. Estuaries 24 (6B), 939.
Luan, H.L., Ding, P.X., Wang, Z.B., Ge, J.Z., Yang, S.L., 2016. Decadal morphological evolution of the Yangtze Estuary in response to river input changes and estuarine engineering projects. Geomorphology 256, 12–23.
Mei, X.F., Dai, Z.J., Wei, W., 2016. Dams induced stage–discharge relationship variations in the upper Yangtze River basin. Hydrol. Res. http://dx.doi.org/10.2166/nh.2015.010.
Milliman, J.D., Shen, H.T., Yang, Z.S., Mead, R.H., 1985. Transport and deposition of river sediment in the Changjiang estuary and adjacent continental shelf. Cont. Shelf Res. 4 (1/2), 37–45.
Nicholls, R.J., Cazenave, A., 2010. Sea-level rise and its impact on coastal zones. Science 328, 1517.
Rossington, S.K., Nicholls, R.J., Stive, M.J.F., Wang, Z.B., 2011. Estuary schematisation in behaviour-oriented modelling. Mar. Geol. 281, 27–34.
Spearman, J.R., Dearnale, M.P., Dennis, J.M., 1998. A simulation of estuary response to training wall construction using a regime approach. Coast. Eng. 33, 71–89.
Syvitski, J.P.M., Vörösmarty, C.J., Kettner, A.J., Green, P., 2005. Impact of humans on the flux of terrestrial sediment to the global coastal ocean. Science 308, 376–380.
Thomas, C.G., Spearman, J.R., Turnbull, M.J., 2002. Historical morphological change in the Mersey Estuary. Cont. Shelf Res. 22, 1775–1794.
Torrence, C., Compo, G.P., 1998. A practical guide to wavelet analysis. Bull. Am. Meteorol. Soc. 79 (1), 61–78.
van der Wal, D., Pye, K., 2003. The use of historical bathymetric charts in a GIS to assess morphological change in estuaries. Geogr. J. 169 (1), 21–31.
van der Wal, D., Pye, K., Neal, A., 2002. Long-term morphological change in the Ribble Estuary, northwest England. Mar. Geol. 189, 249–266.
van der Wegen, M., Dastgheib, A., Roelvink, J.A., 2010. Morphodynamic modeling of tidal channel evolution in comparison to empirical PA relationship. Coast. Eng. 57 (9), 827–837.
Wei, W., Tang, Z.H., Dai, Z.J., Lin, Y.F., Ge, Z.P., Gao, J.J., 2015. Variations in tidal flats of the Changjiang (Yangtze) Estuary during 1950s–2010s: future crisis and policy implication. Ocean Coast. Manag. 108, 89–96.
Wei, W., Mei, X.F., Dai, Z.J., 2016. Recent morphodynamic evolution of the largest uninhibited island in the Yangtze (Changjiang) estuary during 1998-2014: influence of the anthropogenic interference. Cont. Shelf Res. 124, 83–94.
van der Werf, J., Reinders, J., Van Rooijen, J., Holzhauer, H., Ysebaert, T., 2015. Evaluation of a tidal flat sediment nourishment as estuarine management measure. Ocean Coast. Manag. 114, 77–87.
Yan, H., Dai, Z.J., Li, J.F., 2011. Distributions of sediments of the tidal flats in response to dynamic actions, Yangtze (Changjiang) Estuary. J. Geogr. Sci. 21 (4), 719–732.
Yang, S.L., Friedrichs, C.T., Shi, Z., Ding, P.X., Zhu, J., Zhao, Q.Y., 2003. Morphological response of tidal marshes, flats and channels of the outer Yangtze River mouth to a major Storm. Estuaries 26 (6), 1416–1425.
Yang, S.L., Milliman, J.D., Li, P., Xu, K., 2011. 50,000 dams later: erosion of the Yangtze River and its delta. Glob. Planet. Chang. 75, 14–20.
Yun, C.X., 2004. Recent Development of the Changjiang Estuary. first ed. China Ocean Press, Beijing.
Yun, C.X., 2010. Illustrated Handbook on Evolution of Yangtze Estuary. first ed. China Ocean Press, Beijing.